Conformational Dynamics of Cytochrome P-450$_{cam}$ As Monitored by Photoacoustic Calorimetry†

Carmelo Di Primo,‡,§ Gaston Hui Bon Hoa,§ Eric Deprez,§ Pierre Douzou,§ and Stephen G. Sligar*,‡

Department of Biochemistry, Chemistry and Biophysics, University of Illinois, Urbana, Illinois 61801, and INSERM-INRA U310, Institut de Biologie Physico-Chimique, 13 rue Pierre et Marie-Curie, 75005 Paris, France

Received December 7, 1992

ABSTRACT: Conformational transitions of cytochrome P-450$_{cam}$ following the dissociation of CO from the ferrous heme were investigated by using photoacoustic calorimetry. The effect of substrate association on the acoustic signal was also examined. Results show that the conformational dynamics of cytochrome P-450$_{cam}$ substrate-free protein occur faster than 10 ns, which is the time scale of the instrument response. The enthalpy and volume change for the dissociation reaction are 2.2 kcal mol^{-1} and 1.8 mL mol^{-1}, respectively. Upon addition of camphor, the reaction is markedly slowed. An intermediate is formed whose lifetime is 130 ns at 17 °C. The overall enthalpy and volume changes are −15.9 kcal mol^{-1} and 10.3 mL mol^{-1}, respectively. These results, together with published transient Raman spectra [Wells, A. V., Pusheng, L., Champion, P. M., Martinis, S. A., & Sligar, S. G. (1992) *Biochemistry 31*, 4384–4393] suggest that camphor leaves the heme pocket concomitant with the photoinduced expulsion of CO into the solvent and induces a considerable conformational change in the protein.

Cytochrome P-450$_{cam}$, a soluble globular hemoprotein from *Pseudomonas putida*, catalyzes the hydroxylation of camphor, which can be utilized as sole carbon source by the organism. This protein, since its isolation in the late 1950's, has been widely studied as a model for P-450 monooxygenases, which play key roles in mammalians, plants and insects (Gunsalus et al., 1987; Unger et al., 1986; Ortiz de Montellano, 1986).

The three-dimensional X-ray structure of cytochrome P-450$_{cam}$ has been determined in both the structure-free (Poulos et al., 1986) and substrate-bound (Poulos et al., 1985, 1987) forms as well as when complexed with other ligands (Poulos & Howard, 1987; Raag & Poulos, 1989). The active site is entirely buried inside the protein with little or no direct solvent access. One of the most interesting features of the structure is the absence of an apparent access channel for camphor. Clearly the protein undergoes important conformational changes to allow the entrance of the substrate or the exit of the product.

Despite rich literature on cytochrome P-450$_{cam}$, little is known about the molecular motions of this protein in relation to the binding of its substrate, camphor, or smaller molecules such as CO and O_2. The photochemistry of cytochrome P-450$_{cam}$ has been characterized to some extent (Shimada et al., 1979; Imai et al., 1982; Mitani et al., 1985; Wells et al., 1992), but compared to myoglobin, there is no information about the energetics of short-lived species, in the nanosecond to microsecond time scale.

The recent development of the time-resolved photoacoustic calorimetry (Rothberg et al., 1983; Rudzki, 1985; Peters et al., 1991) allows monitoring protein dynamics such as those that might be coupled to ligand or substrate egress from the active site. Previous works have already shown that small changes in volume and enthalpy can be detected in the nanosecond to microsecond time scale, in aqueous medium (Westrick et al., 1990; Marr & Peters, 1991). We present in this paper the quantitation of structural changes of cytochrome P-450$_{cam}$ following the photodissociation of CO from the ferrous heme in the presence and absence of substrate.

MATERIALS AND METHODS

Cytochrome P-450$_{cam}$ was generated and purified as previously described (Gunsalus & Wagner, 1978). Substrate-free protein was obtained by passage of one sample of pure concentrated protein through a Sephadex G-25 column previously equilibrated at 4 °C with the same buffer used for the experiments, 50 mM Tris-HCl (Sigma), pH 7.2, at 20 °C. Ferrous CO-bound cytochrome P-450$_{cam}$ was prepared by bubbling CO in the sample (1-mL solution) during at least 15 min and then reduced with a few crystals of sodium dithionite (Sigma). The cytochrome P-450$_{cam}$–CO–substrate tertiary complex was prepared by adding camphor at a final concentration of 0.5 mM and 240 mM potassium chloride.

The instrument developed in our laboratory is inspired from those previously described (Rothberg et al., 1983; Rudzki, 1985, Peters & Snyder, 1988) and uses a Laser Science nitrogen-pumped dye laser operating at 536 nm, with a 3-ns pulse width at a 2.5-Hz repetition rate. An output energy of 8 μJ was chosen to be within the linear relationship between the acoustic signal of the CO-bound protein and the energy of the laser. The sample was contained in a standard four clear window quartz cuvette fitted into a brass holder. Two Peltier junctions were used to maintain the temperature within ±0.1 °C. The acoustic waves generated by the pulses were detected by a 1-MHz piezoelectric ceramic transducer (Phillips). Its output voltage was amplified by a Panametric preamplifier and recorded by a Lecroy 940 oscilloscope. The data were then transfered to a Silicon Graphics Iris computer for further analysis by using the program SOUNDATA developed in Urbana.

In order to calibrate the instrument, a compound which converts the absorbed light only into heat deposited in the

† This work was supported by grants from the National Institutes of Health (GM33775 and GM31756), by the Institut National de la Santé et de la Recherche Médicale (U310), and by the Institut National de la Recherche Agronomique. S.G.S. gratefully acknowledges receipt of a Fulbright Fellowship.

* To whom correspondence should be addressed.
‡ University of Illinois.
§ INSERM-INRA U310.

0006-2960/93/0432-3671$04.00/0

medium is used (Peters et al., 1991). Cytochrome P-450$_{cam}$ in its oxidized form was used as a calibration compound since no conformational change is expected upon excitation by the laser. We determined that the oxidation state of the heme iron or the presence of camphor and potassium chloride did not affect the calibration signal. Ferric cytochrome P-450$_{cam}$ in 50 mM Tris-HCl was used as a calibration compound for the experiments with the ferrous CO cytochrome P-450$_{cam}$ form and the oxidized form of the substrate-bound protein as a calibration compound for the experiments with the teritary complex ferrous cytochrome P-450$_{cam}$–CO–substrate. Previous studies have shown that even if the amplitude of the acoustic signal can be corrected for the energy absorbed as $E_{h\nu}(1-10^{-A})$, where $E_{h\nu}$ is the energy of the photon and A the absorbance of the sample, the signal is sensitive in time to variation in absorbance between samples (Rudzki, 1985). We kept the difference in absorbance between the calibration compound and the sample of interest within 0.02 at 536 nm, which is the isosbestic point of the spectra of oxidized cytochrome P-450$_{cam}$ with or without substrate and reduced CO-bound cytochrome P-450$_{cam}$. The concentration of protein currently used was 30–40 μM with a corresponding absorbance of 0.3–0.4.

Our analysis of the photoacoustic signals follows exactly the pioneering work of the Peters group (Peters et al., 1991). The photoacoustic signal, S, generated by the contraction or the expansion of the irradiated sample is given by $S = K\Delta V$, where K is the constant of the instrument response. In proteins, the volume change, ΔV, results from two major contributions. A thermal term, ΔV_{th}, comes from the energy, ΔE, rapidly deposited in the medium during the photoinduced reaction. The second is related to the conformational changes induced by the photochemistry, ΔV_{conf}. These changes are directly related to net changes in the volume of the protein, solvent packing, and/or electrostriction of exposed charges to the solvent. The photoacoustic signal can be written as

$$S = K(\Delta V_{th} + \Delta V_{conf}) = K[(\beta/C_p\rho)\Delta E + \Delta V_{conf}] \quad (1)$$

where β represents the thermal expansion coefficient, C_p the heat capacity, and ρ the density of the solvent.

In order to eliminate K, the constant of the instrument response, $\varnothing$ is defined as the ratio of the signal arising from the sample of interest, S, over the signal of the calibration compound S_{cal}. Assuming that after photodissociation the ligand, CO, diffuses out of the protein with a quantum yield of unity (see Discussion), then

$$\varnothing = S/S_{cal} = (\Delta E/E_{h\nu}) + \Delta V_{conf}/[(\beta/C_p\rho)E_{h\nu}] \quad (2)$$

$\varnothing$ is temperature dependent since β, C_p and ρ are. Defining $F(T) = (\beta/C_p\rho)$, eq 2 becomes

$$E_{h\nu}\varnothing = \Delta E + \Delta V_{conf}/F(T) \quad (3)$$

A study of the photoacoustic signals as a function of the temperature will separate ΔV_{conf} and ΔE. The enthalpy change for the reaction is thus

$$\Delta H = E_{h\nu} - \Delta E$$

The experimental acoustic wave, $E(t)$, results from the convolution of the instrument response, $T(t)$, obtained with the calibration compound, with a time-dependent function, $H(t)$, which describes the decay of the successive photoinduced species (Rudzki, 1985):

$$E(t) = T(t)H(t).$$

Two models were initially assumed to fit the data: a two-state model and a three-state model. The best fit was obtained with the latter:

$$A \xrightarrow{k_1} B \xrightarrow{k_2} C$$

where k_1 and k_2, the kinetic constants, are equal to $1/\tau_1$ and $1/\tau_2$, respectively. The time-dependent function $H(t)$ will have the form:

$$H(t) = \varnothing_1 \exp(-t/\tau_1) + [\varnothing_2\tau_2/(\tau_1 - \tau_2)][\exp(-t/\tau_1) - \exp(-t/\tau_2)] \quad (4)$$

The procedure to find $\varnothing_1$, $\varnothing_2$, τ_1, and τ_2 (Brigham, 1974; Rudzki, 1985), involves the convolution in the time domain of a calculated $H(t)$, assuming a set of $\varnothing_1$, $\varnothing_2$, τ_1, and τ_2, with the instrument response, $T(t)$. The calculated wave, $C(t)$, is then compared to the observed wave, $E(t)$. The fit is evaluated by the square sum of the residuals after each set of $\varnothing$ and τ. In our model, we assumed that τ_1 was much faster than the time response of the instrument and could not be temporally resolved. Then τ_1 was held constant and only $\varnothing_1$, $\varnothing_2$, and τ_2 were varied. As noted previously (Rudzki, 1985), our attempts to deconvolute the instrument response function from the observed signal using Fourier transforms or polynomial curve fitting procedures did not yield accurate results.

RESULTS

The photoacoustic spectra of cytochrome P-450$_{cam}$, at 17 °C, for different binding states of the heme pocket are presented in Figure 1a. The oxidized form of the protein was used as a calibration compound to generate the instrument response, $T(t)$. In this case the energy absorbed by the sample during the pulse of light is manisfested as heat deposited in the medium. The signal obtained corresponds to the fastest response detectable by the instrument. The theory of photoacoustic calorimetry (Peters et al., 1991) predicts that if chemistry occurs faster than the time scale of the instrument response, the reaction will not be temporally resolved but the instrument will still be sensitive to changes in enthalpy and volume within the system. If the photoinduced reaction occurs in the time scale of the instrument, roughly 10 ns to 30 μs, temporally resolved thermodynamic information can be obtained. The amplitude of the signal for ferrous CO-bound cytochrome P-450$_{cam}$ substrate-free is higher than that generated with the calibration compound. The signal is not shifted in time as it was reported for carbon monoxide photolysis from sperm whale myoglobin (Rudzki, 1985; Westrick et al., 1990). This clearly means that all photochemical events in the substrate-free protein are occurring faster than the time scale of the instrument response. When camphor is present, however, the signal increases in amplitude and is significantly shifted in time.

The photoacoustic signal in the same conditions but at lower temperature, 2.5 °C, are reported in Figure 1b. In pure water, the thermal expansion coefficient, β, is equal to zero near 4 °C. Because of the concentrations of protein used, typically 30–40 μM in 50 mM Tris–HCl buffer, C_p, ρ, and β are slightly altered from the values of pure water. The new values were determined as described elsewhere (Westrick et al., 1990). The calibration compound used, oxidized cytochrome P-450$_{cam}$, does not show significant signal at 2.5 °C. This result demonstrates that only thermal energy deposited in the medium contributes to the signal observed at higher temperature. On the contrary, for the CO-bound forms, with or without substrate, a signal is still detected at 2.5 °C. Since the thermal contribution is eliminated at this temperature, the observed signals arise from photoinduced conformational events. Again the signal of the tertiary complex appears shifted in time with

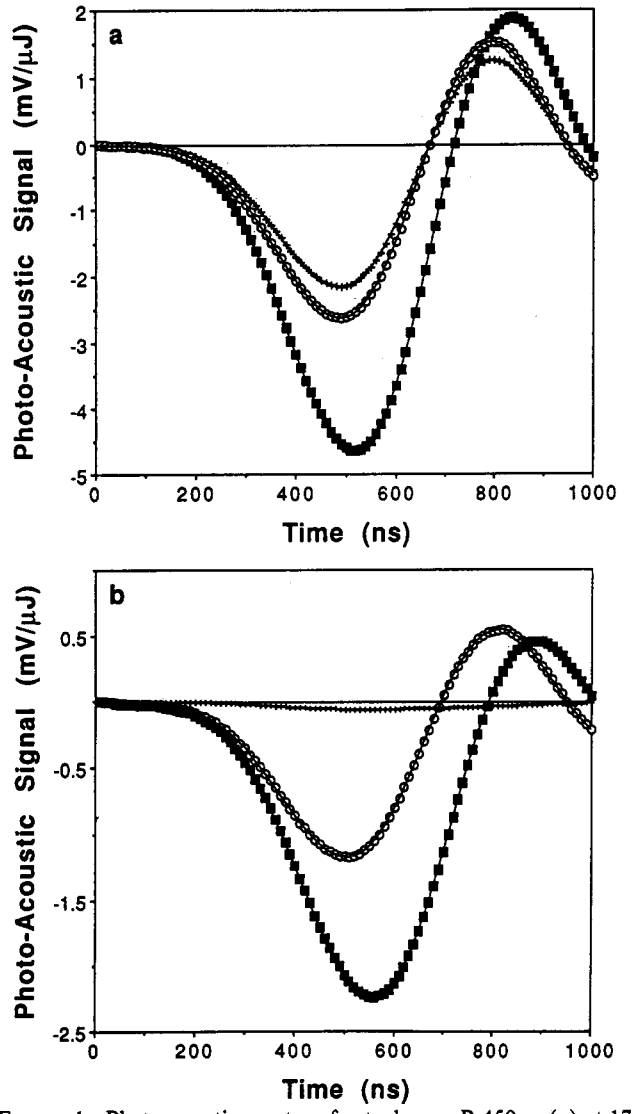

FIGURE 1: Photoacoustic spectra of cytochrome P-450$_{cam}$ (a) at 17 °C and (b) at 2.5 °C. Experimental conditions are described under Materials and Methods. (+) Cytochrome P-450$_{cam}$ oxidized (calibration compound). (O) Ferrous cytochrome P-450$_{cam}$–CO. (■) Ferrous cytochrome P-450$_{cam}$–CO–camphor.

higher amplitude compared to the substrate-free protein. However, the signs of these signals were not changed as they were for carboxymyoglobin (Rudzki, 1985).

Since ferrous CO-bound cytochrome P-450$_{cam}$ substrate-free signal is not shifted in time, no kinetic information is available. The fit which gives the unique Ø for the reaction of dissociation as a function of $C_p\rho/\beta$ is the ratio of the integrated area of the CO sample signal to the integrated area of the calibration compound signal. The corresponding plot is shown in Figure 2a. The volume and enthalpy changes deduced are 1.8 ± 0.1 mL mol^{-1} and 2.2 ± 0.9 kcal mol^{-1}, respectively. The actual meaning of these numbers considering that only 5% of the CO molecules photodissociated diffuse out of the protein pocket will be discussed in the next section.

The procedure used to fit the data for the experiments with the tertiary complex cytochrome P-450$_{cam}$–CO–substrate involves the convolution of the instrument response, $T(t)$, with the heat function, $H(t)$. $E_{h\nu}Ø_1$ and $E_{h\nu}Ø_2$ as a function of $C_p\rho/\beta$ are reported in Figure 2, panels b and c, for the first and the second step, respectively. The parameters deduced from these plots are ΔV_1 = 4.4 ± 0.4 mL mol^{-1}, ΔH_1 = 12.4 ± 3.1 kcal mol^{-1} and ΔV_2 = 5.9 ± 0.4 mL mol^{-1}, ΔH_2 = −27.9 ± 3.2 kcal mol^{-1} for the first and the second step, respectively.

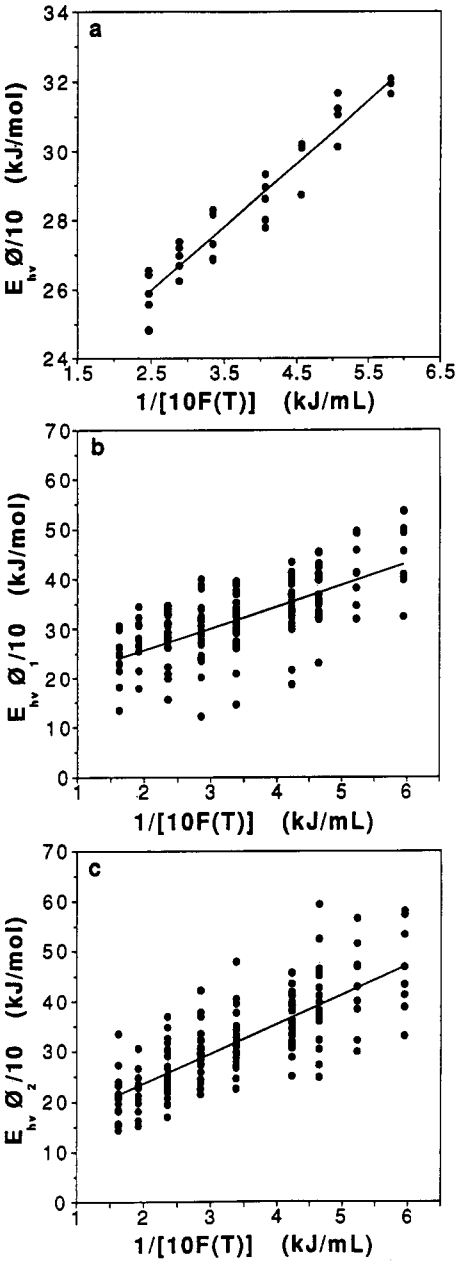

FIGURE 2: Plots of the $E_{h\nu}Ø$ versus $1/[10F(T)]$ (a) for ferrous cytochrome P-450$_{cam}$–CO, (b) for the first step of the reaction with the tertiary complex ferrous cytochrome P-450$_{cam}$–CO–camphor, and (c) for the second step of the reaction with the tertiary complex ferrous cytochrome P-450$_{cam}$–CO–camphor.

In Figure 3 we report an example of the net residuals here for the 17 °C data set, assuming the fit parameters $Ø_1$ = 1.235, $Ø_2$ = 1.335, and τ_2 = 132.5 ns. The fit is indistinguishable from the observed signal.

In the analysis of the data, we assumed a two-step model. Kinetic information is only available for the second step. In Figure 4 we present a plot of the corresponding kinetic constant as a function of $-1/RT$ between 26 and 10 °C. The activation parameters deduced are ΔH_2^* = 12.0 ± 0.9 kcal mol^{-1} and ΔS_2^* = 13.9 ± 3.1 cal mol^{-1} K^{-1}. Table I summarizes the enthalpy and volume changes as well as the activation parameters for cytochrome P-450$_{cam}$. Finally in Figure 5 we show an energy landscape for the tertiary complex ferrous CO–cytochrome P-450$_{cam}$ substrate-bound as derived from the experimental data.

DISCUSSION

The photochemistry of CO-bound hemoproteins has been extensively documented in recent years and has provided

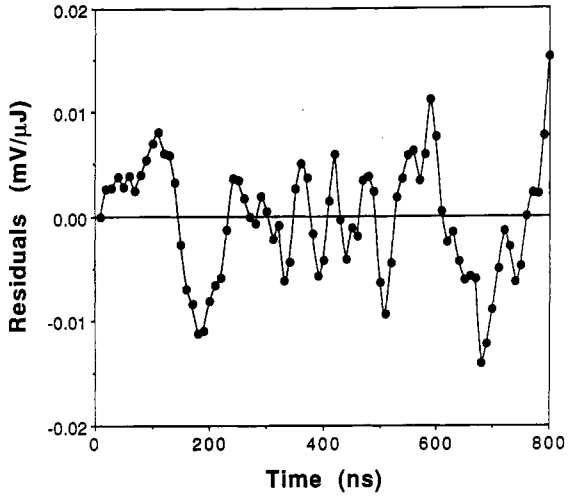

FIGURE 3: Plot of the residuals corresponding to the difference between the calculated wave and the observed wave obtained with the tertiary complex ferrous cytochrome P-450$_{cam}$–CO–camphor, assuming $\emptyset_1$ = 1.235, $\emptyset_2$ = 1.335, and τ_2 = 132.5 ns, at 17 °C. The procedure to find these parameters is described under Materials and Methods.

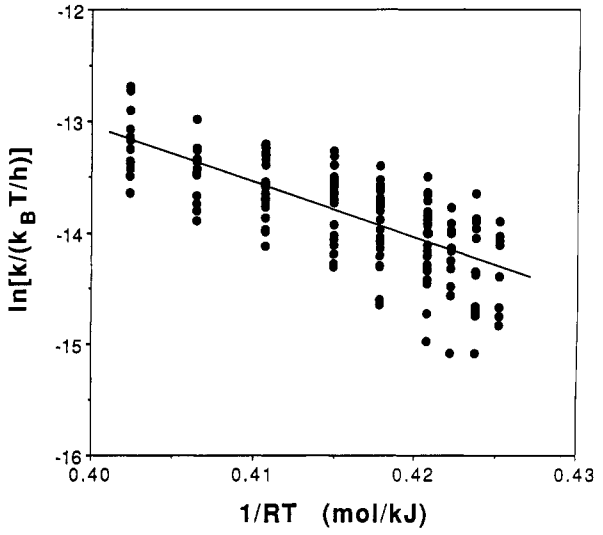

FIGURE 4: Arrhenius plot for the second step of the dissociation of CO from cytochrome P-450$_{cam}$ in the presence of camphor. The experiments were performed between 26 and 10 °C.

interesting insights about protein motions in relation to their biological functions. In this respect myoglobin has been, and remains, the most studied protein (Antonini & Brunori, 1971). Its highly resolved three-dimensional X-ray structure and apparent simplicity, its good stability against physical-chemical agents such as pH, temperature, and pressure, its well-characterized biological properties, and more recently the possibility to achieve site-directed mutagenesis (Springer & Sligar, 1987) have made myoglobin the adequate candidate as a model for the investigation of protein dynamics (Frauenfelder et al., 1991). After more than 15 years of work, the key question remains to understand how small ligands such as CO or O_2 reach the active site through the protein matrix and escape from the heme pocket.

Cytochrome P-450$_{cam}$ has been also very well characterized. Immediately, the system appears more complex than myoglobin. The catalytic function requires two more proteins which transfer electrons (Sligar & Gunsalus, 1976). The three-dimensional X-ray structure clearly shows two well-defined regions of secondary structure (Poulos et al., 1985), one composed primarily of α-helix and the other of random coil and β-sheets. The heme pocket is completely buried in the protein between these two domains. The substrate, camphor, couples the two structural regions of the protein via hydrophobic interactions and the tyrosine 96/camphor hydrogen bond. This coupling is well known to play an important role in hydroxylation regiospecificity (Atkins & Sligar, 1989), substrate affinity (Atkins & Sligar, 1988), cation cooperativity (Di Primo et al., 1990a), and stability against inactivation by hydrostatic pressure (Di Primo et al., 1990b). Compared with myoglobin, cytochrome P-450$_{cam}$ is more responsive to physical–chemical perturbations (Fisher et al., 1985; Marden & Hui Bon Hoa, 1982).

The ferrous CO-bound form of the protein presents an unusual 450-nm Soret band red-shifted by 30 nm relative to that of most other ferrous CO-bound hemoproteins (Garfinkel, 1958; Klingenberg, 1958). This feature is attributed to the proximal cystein ligand in P-450 instead of an axial histidine ligand for globins. The Soret band at 450 nm is not sensitive upon addition of camphor. On the contrary, FTIR spectra of the stretch frequencies of the C–O bond cytochrome P-450$_{cam}$ are clearly sensitive to the presence of camphor (Jung & Marlow, 1987; O'Keefe et al., 1978).

The decision to use photoacoustic calorimetry as a tool to investigate molecular dynamics in cytochrome P-450$_{cam}$ was motivated by the goal to understand the mechanism by which the substrate molecule accesses the buried active site. The X-ray structure and associated thermal factors suggest that the protein probably undergoes large conformational changes during binding of metabolizable substrates. These motions, here triggered by the photoinduced dissociation of CO, could be detected by photoacoustic calorimetry. The results obtained for substrate-free ferrous CO-bound cytochrome P-450$_{cam}$ will be discussed first.

Camphor-Free Form. The energetics and the volume changes for the photoinduced dissociation of CO from cytochrome P-450$_{cam}$, in the nanosecond to microsecond time scale, were not known prior this study. It has been shown that the photoinduced dissociation of CO from the heme–iron occurs within femtoseconds with a quantum yield of unity (Petrich et al., 1988). Smaller values reported for globular proteins on longer time scale are attributed to fast geminate recombination event. Shimada and co-workers (Shimada et al., 1979), who first reported the photodissociation of CO from cytochrome P-450$_{cam}$, found that only 6% and 100% of the CO photodissociated diffused out of the protein for the substrate-free and -bound ferrous CO-bound complexes, respectively, in good agreement with our determination of 5 ± 1% and 100% for the substrate-free and -bound forms. The signals at 2.5 °C where the thermal contribution is minimal are interesting. The amplitude of the signal generated without camphor is half the amplitude of the signal obtained with the substrate. This result is surprising considering that at this temperature only 5% of the CO molecules photodissociated leave the substrate-free protein. Obviously other contributions are also being measured.

Even if the reaction cannot be temporally resolved, the photoacoustic calorimeter is still sensitive to the heat rapidly deposited in the medium and volume changes within the system. If we assume that the photoinduced dissociation of CO in the absence of camphor can be also described by a two-step model, the geminate pair being the intermediate formed, the ΔH and ΔV determined here describe not only the diffusion of the CO molecule out of the protein but also the formation of the geminate pair and the fast geminate recombination. Then ΔH measured would be equal to $\Delta H_1 - (1 - Q)\Delta H_1 + Q\Delta H_2$, where ΔH_1 is the enthalpy change for the formation of the geminate pair, ΔH_2 is the enthalpy change for the formation of the CO-free protein, and Q is the quantum yield of CO

Table I: Enthalpy, Volume Changes, and Activation Parameters for Cytochrome P-450$_{cam}$

			ΔV^a		ΔH^b	
P-450–CO			1.8 ± 0.1		2.2 ± 0.9	
	ΔV^a	$\Delta H_1{}^b$	$\Delta V_2{}^a$	$\Delta H_2{}^b$	$\Delta H_2{}^{\ddagger b}$	$\Delta S_2{}^{\ddagger c}$
P-450–CO +camphor	4.4 ± 0.4	12.4 ± 3.1	5.9 ± 0.4	−27.9 ± 3.2	12.0 ± 0.9	13.9 ± 3.1

[a] mL mol^{-1}. [b] kcal mol^{-1}. [c] cal mol^{-1} K^{-1}

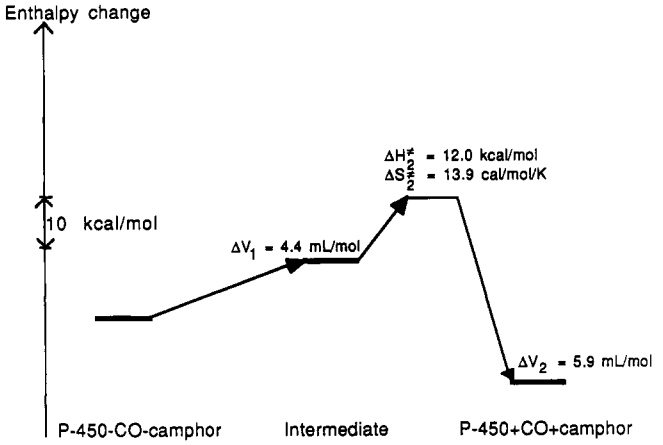

FIGURE 5: Energy landscape of the photoinduced dissociation of CO from cytochrome P-450$_{cam}$ in the presence of camphor.

dissociation equal to 0.05. A similar formula could be written for the ΔV measured. Regrettably, we do not know the enthalpy and volume changes for the formation of the geminate pair in cytochrome P-450$_{cam}$. Is the intermediate formed in the presence of camphor the geminate pair itself? Is its formation independent of the presence of camphor? Then could we use ΔH_1 and ΔV_1 obtained in this condition to deduced ΔH_2 and ΔV_2 without camphor? Our results cannot answer these questions.

In an attempt to clarify the meaning of the photoacoustic signals, we determined spectroscopically the overall enthalpy of the reaction. The variation of the equilibrium constant as a function of temperature gives an enthalpy change for the dissociation of CO equal to 6.5 ± 1.1 kcal mol^{-1} in the absence of camphor.

The low quantum yield reported for the substrate-free protein poses an interesting problem. When the heme iron–CO bond is broken, only 5% of bimolecular recombination is observed, which suggests that 95% of the CO molecules dissociated do not escape into the solvent and recombinate rapidly with the heme–iron. Above 270 K, in aqueous medium, most of the CO flashed from sperm-whale myoglobin leaves the protein (Doster et al., 1982; Henry et al., 1983). The three-dimensional structures of cytochrome P-450$_{cam}$ (Poulos et al., 1985) and myoglobin (Kendrew et al., 1960; Phillips, 1981) show that the active site of the latter is tightly packed while for the former it defines a cavity which accommodates water molecules or 10 carbons of the substrate molecule. Other evidences for a more open active site come from FTIR spectroscopy of these two proteins where at least five stretch bands have been detected for camphor-free cytochrome P-450$_{cam}$ (O'Keefe et al., 1978; Jung & Marlow, 1987) while only three are present for myoglobin (Ansari et al., 1987). Will a more open active site favor the escape of the ligand into the solvent or on the contrary force it to stay close to the heme–iron favoring the fast geminate recombination? In a more open active site, the ligand could wander after photo-induced dissociation throughout the heme pocket as, for example, a "separated pair" according to a model proposed earlier (Jongeward et al., 1988) and then could rebind to the iron atom. In this model, the geminate pair would exist at least in two forms, the "contact pair" formed within femtoseconds to picoseconds and the "separated pair" which reacts with a 10^7–10^8 s^{-1} rate constant, close to the lower limit of time resolution of our instrument. The increase in the quantum yield when camphor is bound contrasts with what one could expect when the steric constraints inside the heme pocket increase by the presence of a substrate or increasing size of amino acids side chains, as it was also reported (Berinstain et al., 1990; Carver et al., 1990).

Camphor-Bound Form. The question is to understand why in the presence of camphor the signal is time shifted relative to the calibration compound and its amplitude higher. Previous work has shown that the rate constant for the reaction of CO with cytochrome P-450$_{cam}$ were decreased up to 150-fold upon addition of the substrate. This was attributed to steric constraints that CO must overcome to bind the iron (Peterson et al., 1971; Peterson & Griffin, 1972; Pederson et al., 1976; Mims et al., 1983). The three-dimensional X-ray structure clearly shows that camphor is displaced when CO binds (Raag & Poulos, 1989a). In our experiments an intermediate is formed within the time scale of the instrument response with 130-ns lifetime and larger changes in enthalpy and volume as reported in Table I. As previously mentioned, its nature is unknown even if the model assumed implicitly suggests that it is close to that of a geminate pair. The second step of the reaction is slow enough to be detected within the time scale of the instrument response. Does this reflect a migration process of CO and/or camphor through the protein matrix or a relaxation process after CO and camphor have left the active site as it was proposed for myoglobin (Westrick et al., 1990)? The hypothesis of the exit of camphor pushed by the CO molecule is attractive. The slow and large dynamics expected to open a channel for the substrate could then explain the origin of the phase shift and the larger amplitude of the signals. Naturally, our results cannot definitively tell whether or not the final state of the photoinduced reaction is a camphor-free form. A recent report, however, strongly supports this idea. Raman spectroscopy of a photolysed tertiary ferrous complex CO–substrate–cytochrome P-450$_{cam}$ gave direct evidence for the presence of substrate-free forms (Wells et al., 1992).

The overall volume change, $\Delta V_{1+2} = 10.3$ mL mol^{-1}, suggests that the protein–solvent system is larger in its final state than in the initial state. Camphor plays a key role in linking the two dynamic domains of secondary structure and substantially increasing the stability of the protein (Di Primo et al., 1990b). Although the three-dimensional X-ray structure does not show significant changes in the overall structure of the protein when camphor binds, the volume changes probably reflect reorganization of protein–solvent ratios other than just changes in the physical volume of the structure. ΔV is a complex parameter the variations of which have also been attributed to changes in hydration (Weber & Drickamer, 1983; Rodgers & Sligar, 1991; Di Primo et al., 1990b). The fixation/dissociation of camphor involves movement of water molecules (Fisher & Sligar, 1987; Raag & Poulos, 1989b). This, as

well as electrostriction around transiently exposed charged groups, could contribute to the measured volume.

The negative $\Delta H_{1+2} = -15.9$ kcal mol^{-1} is different from the overall enthalpy change measured spectroscopically, 5.5 $\pm$ 0.9 kcal mol^{-1}. If camphor really leaves the protein when CO is dissociated, the negative enthalpic contribution from the dissociation of camphor, roughly -10 kcal mol^{-1} (data not published), could be also measured by photoacoustic calorimetry. The meaning of the activation parameters deduced from the variation of the kinetic constant as a function of $1/RT$ for the second step of the reaction is not clear. However, in such a complex system, contributions like release of water molecules into the solvent after relaxation of the structure could be responsible for the positive entropy of activation.

In summary, increase in the amplitude of the signals for ferrous CO-bound cytochrome P-450$_{cam}$ substrate-free and -bound compared to the calibration compound involves structural reorganization of the protein during the photoinduced dissociation of CO. Camphor clearly affects the dynamics of the protein. A reaction not temporally resolved becomes slow enough to be detected as illustrated by the phase shift of the photoacoustic signal. Camphor would leave the heme pocket concomitant with the dissociation of CO and involves important conformational changes within the protein linked to an opening of an access channel.

ACKNOWLEDGMENT

We gratefully thank M. C. Marden from the Institut National de la Santé et de la Recherche Médicale, U299, for the determination of the quantum yields. We also thank J. M. Glandières and C. Zentz from the Université de Paris 7 for helpful discussions.

REFERENCES

Ansari, A., Berendzen, J., Braunstein, D., Cowen, B. R., Frauenfelder, H., Hong, M. K., Iben, I. E. T., Johnson, J. B.; Ormos, P., Sauke, T. B., Scholl, R., Schulte, A., Steinbach, P. J.; Vittitow, J., & Young, R. D. (1987) *Biophys. Chem. 26*, 337–355.

Antonini, E., & Brunori, M. (1971) *Hemoglobin and Myoglobin in Their Reaction with Ligands*, North Holland, Amsterdam.

Atkins, W. M., & Sligar, S. G. (1988) *J. Biol. Chem. 263*, 18842–18849.

Atkins, W. M., & Sligar, S. G. (1989) *J. Am. Chem. Soc. 111*, 2715–2717.

Berinstain, A. B.; English, A. M., Hill, B. C., & Sharma, D. (1990) *J. Am. Chem. Soc. 112*, 9649–9651.

Brigham, E. O., Jr. (1974) *The Fast Fourier Transform*, Prentice-Hall, Englewood Cliffs, NJ.

Carver, T. E., Rohlfs, R. J., Olson, J. S., Gibson, Q. H., Blackmore, R. S., Springer, B. A., & Sligar, S. G. (1990) *J. Biol. Chem. 265*, 20007–20020.

Di Primo, C., Hui Bon Hoa, G., Douzou, P., Sligar, S. G. (1990a) *J. Biol. Chem. 265*, 5361–5363.

Di Primo, C., Hui Bon Hoa, G., Douzou, P., Sligar, S. G. (1990b) *Eur. J. Biochem. 193*, 383–386.

Doster, W., Neece, D., Bowne, S. F., Dilorio, E. E., Eisenstein, L., Frauenfelder, H., Reinisch, L., Shyamsunder, E., Winterhalter, K. H., & Yue, K. T. (1982) *Biochemistry 21*, 4831–4839.

Fisher, M. T., Scarlata, S. F., & Sligar, S. G. (1985) *Arch. Biochem. Biophys. 240*, 456–463.

Fisher, M. T., Scarlata, S. F., & Sligar, S. g. (1987) *Biochemistry 26*, 4797–4803.

Frauendfelder, H., Sligar, S. G., & Wolynes, P. G. (1991) *Science 254*, 1598–2603.

Garfinkel, D. (1958) *Arch. Biochem. Biophys. 77*, 493–509.

Gunsalus, I. C., & Wagner, G. C. (1978) *Methods Enzymol. 52*, 116–188.

Gunsalus, I. C., Koga, H., & Sligar, S. G. (1987) *Four Decades of P-450*, Proceedings of the Yamada Conference (Sato, R., Ed.) pp 142–149, Yamada Foundation, Tokyo.

Henry, E. R., Sommer, J. H. Hofrichter, J., & Eaton, W. (1983) *J. Mol. Biol, 166*, 443–451.

Imai, Y., Iizuka, T., & Ishimura, Y. (1982) *J. Biochem. (Tokyo) 92*, 67–75.

Jongeward, K. A., Madge, D., Taube, D. J., Marsters, J. C., Traylor, T. G., & Sharma, V. S. (1988) *J. Am. Chem. Soc. 110*, 380–387.

Jung, C., & Marlow, F. (1987) *Stud. Biophys. 120*, 241–251.

Kendrew, J. C., Dickerson, R. E., Strandberg, B. E., Hart, R. G., Davies, D. R., Phillips, D. C., & Shore, V. C. (1960) *Nature (London) 185*, 422–427.

Klingenberg, M. (1958) *Arch. Biochem. Biophys. 75*, 376–386.

Marden, M. C., & Hui Bon Hoa, G. (1982) *Eur. J. Biochem. 129*, 111–117.

Marr, K., & Peters, K. S. (1991) *Biochemistry 30*, 1254–1258.

Mims, M. P., Porras, A. G., Olson, J. S., Noble, R. W., & Peterson, J. A. (1983) *J. Biol. Chem. 258*, 14219–14232.

Mitani, F., Iizuka, T., Shimada, H., Ueno, R., & Ishimura, Y. (1985) *J. Biol. Chem. 260*, 12042–12048.

O'Keefe, D. H., Ebel, R. E., Peterson, J. A., Maxwell, J. C., & Caughley, W. S. (1978) *Biochemistry 17*, 5845–5852.

Ortiz de Montellano, P. (1986) *Cytochrome P-450*, Plenum Press, New York.

Peters, K. S., & Snyder, G. J. (1988) *Science 241*, 1053–1057.

Peters, K. S., Watson, T., & Marr, K. (1991) *Annu. Rev. Biophys. Biophys. Chem. 20*, 343–362.

Pederson, T. C., Austin, R. H., & Gunsalus, I. C. (1976) in *P450$_{cam}$–Putidaredoxin Complex in Microsomes and Drug Oxidations* (Ullrich, V., Ed.) pp 275–283, Pergamon Press, Oxford.

Peterson, J. A., & Griffin, B. W. (1972) *Arch. Biochem. Biophys. 151*, 427–433.

Peterson, J. A., Ullrich, V., & Hildebrandt, A. G. (1971) *Arch. Biochem. Biophys. 145*, 531–542.

Petrich, J., W., Poyart, C., & Martin, J. L. (1988) *Biochemistry 27*, 4049–4060.

Phillips, S. E. V. (1981) *The X-ray Structure of Deoxy-Mb (pH 8.5) at 1.4 Å Resolution*, Brookhaven Protein Data Bank.

Poulos, T. L., & Howard, A. J. (1987) *Biochemistry 26*, 8165–8174.

Poulos, T. L., Finzel, B. C., Gunsalus, I. C., Wagner, G. C., & Krant, J. (1985) *J. Biol. Chem. 260*, 16122-16130.

Poulos, T. L., Finzel, B. C., & Howard, A. J. (1986) *Biochemistry 25*, 5314–5322.

Poulos, T. L., Finzel, B. C., & Howard, A. J. (1987) *J. Mol. Biol. 195*, 687–700.

Raag, R., & Poulos, T. L. (1989a) *Biochemistry 28*, 7586–7592.

Raag, R., & Poulos, T. L. (1989b) *Biochemistry 28*, 917–922.

Rodgers, K. K., & Sligar, S. G. (1991) *J. Mol. Biol. 221*, 1453–1460.

Rothberg, L. J., Simon, J. D., Berstein, M., & Peters, K. S. (1983) *J. Am. Chem. Soc. 105*, 3464–3468.

Rudzki, J. E. (1985) Ph.D. Thesis, Harvard University, Cambridge MA.

Shimada, H., Iizuka, T., Ueno, R., & Ishimura, Y. (1979) *FEBS Lett. 98*, 290–294.

Sligar, S. G., & Gunsalus, I. C. (1976) *Proc. Natl. Acad. Sci. U.S.A. 73*, 1078–1082.

Springer, B. A., & Sligar, S. G. (1987) *Proc. Natl. Acad. Sci. U.S.A. 84*, 8961–8965.

Unger, B., Gunsalus, I. C. & Sligar, S. G. (1986) *Pseudomonas cytochromes P-450. The Bacteria X* (Sokatch, J., Ed.) pp 557–587, Academic Press, New York.

Weber, G., & Drickamer, H. G. (1983) *Q. Rev. Biophys. 16*, 89–112.

Wells, A. V., Pusheng, L., Champion, P. M., Martinis, S. A., & Sligar, S. G. (1992) *Biochemistry 31*, 4384–4393.

Westrick, J. A., Peters, K. S., Ropp, J. D., & Sligar, S. G. (1990) *Biochemistry 29*, 6741–6746.